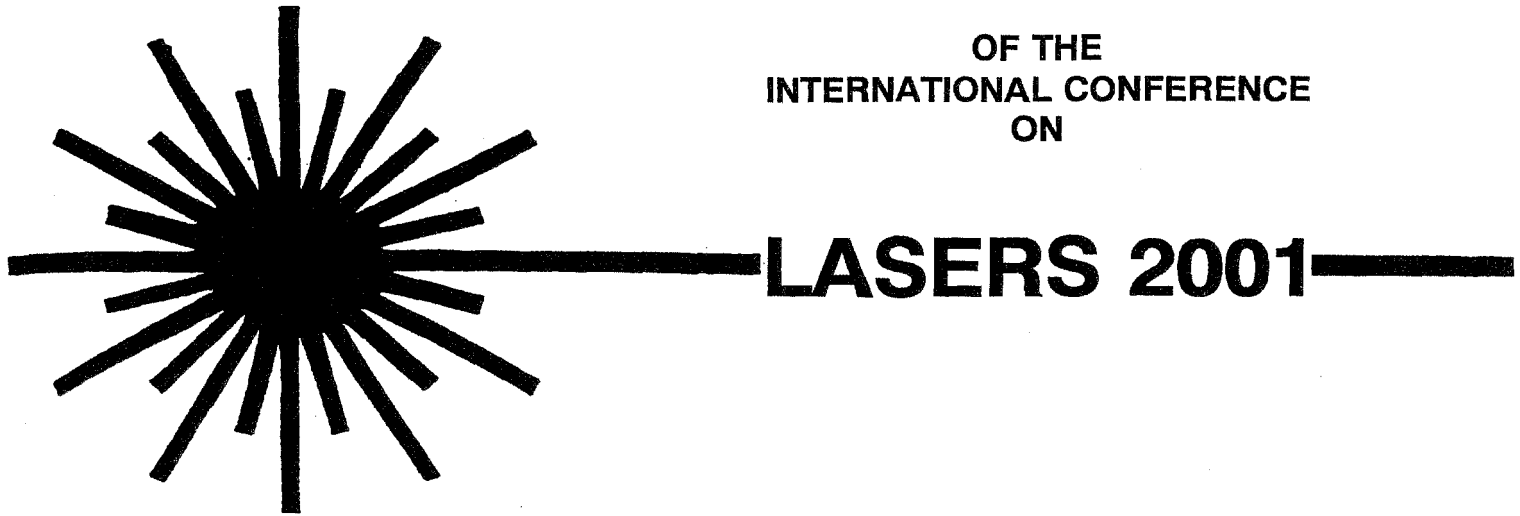


***PROCEEDINGS***

**OF THE  
INTERNATIONAL CONFERENCE  
ON**



**TUCSON, ARIZONA**

**DECEMBER 3-7, 2001**

**V.J. CORCORAN & T.A. CORCORAN**  
*Editors*

***CONFERENCE SPONSORED BY***  
**THE SOCIETY FOR OPTICAL & QUANTUM ELECTRONICS**

**STS PRESS • McLEAN, VA • 2002**

# EFFECTS OF TEMPERATURE ON SHARP SPECTRAL LINES OF Nd<sup>3+</sup> IN LaSc<sub>3</sub>(BO<sub>3</sub>)<sub>4</sub>

Felipe S. Salinas, Joey A. French, Francisco Castano, and Dhiraj K. Sardar  
 Department of Physics and Astronomy  
 The University of Texas at San Antonio  
 San Antonio, Texas 78249

## Abstract

Effects of temperature on widths and shifts of the spectral lines of Nd<sup>3+</sup> in LaSc<sub>3</sub>(BO<sub>3</sub>)<sub>4</sub> have been investigated. The spectral lines corresponding to the inter-Stark transitions R<sub>1</sub> → Y<sub>3</sub> (1062 nm) and R<sub>1</sub> → Z<sub>4</sub> (1344 nm) within the <sup>4</sup>F<sub>3/2</sub> → <sup>4</sup>I<sub>11/2</sub> and <sup>4</sup>F<sub>3/2</sub> → <sup>4</sup>I<sub>13/2</sub> transitions, respectively, have been studied. The widths of these lines and their shifts have been measured as a function of temperature. The spectral linewidths of both transitions are found to increase with increasing temperature. The 1344 nm line shifts to the longer wavelengths, whereas the 1062 nm line shifts to the shorter wavelengths. The phonon-ion interaction theory has been employed to explain the temperature dependencies of widths and shifts.

## Introduction

A detailed characterization of the temperature dependencies of widths and shifts of the fluorescence lines due to the R<sub>1</sub> → Y<sub>3</sub> (1062 nm) and R<sub>1</sub> → Z<sub>4</sub> (1344 nm) inter-Stark transitions of Nd<sup>3+</sup> ions in LSB host is presented in this article. These transitions are shown in the inter-stark energy level diagrams in Figs. 1 and 2, respectively. The observed temperature dependencies of the spectral widths and shifts of these lines are explained with the help of the theory of phonon-ion interaction as a perturbation in which the Debye phonon distribution for the crystalline host lattice is assumed. The theory of phonon-induced relaxation processes was employed to explain the thermal behavior of widths and shifts of sharp spectral lines of the rare earth ions in crystalline host lattices.<sup>1-4</sup>

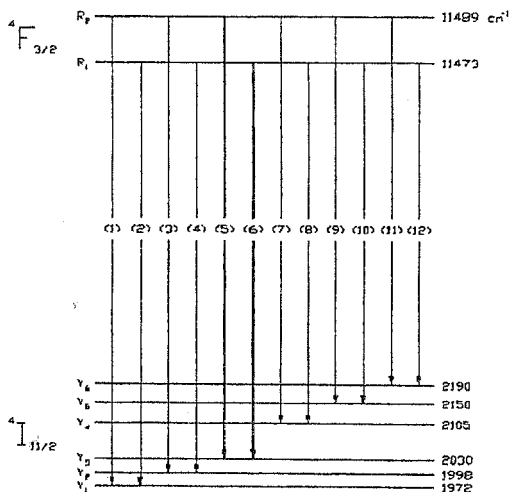


Figure 1. Energy level diagram of Nd<sup>3+</sup> in LSB for the inter-Stark transitions between the <sup>4</sup>F<sub>3/2</sub> and <sup>4</sup>I<sub>11/2</sub> manifolds.

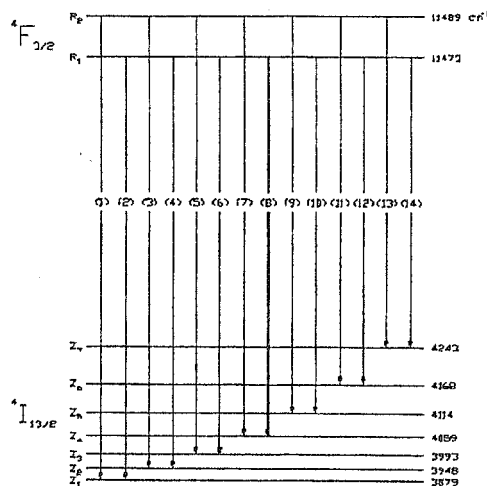


Figure 2. Energy level diagram of Nd<sup>3+</sup> in LSB for the inter-Stark transitions between the <sup>4</sup>F<sub>3/2</sub> and <sup>4</sup>I<sub>13/2</sub> manifolds.

The statistical nature of the strains in solids is random, thereby giving rise to an inhomogeneous broadening which predicts a Gaussian line shape. The linewidths increased with increasing crystal temperature. The temperature-dependent line broadening as well as shift can be attributed to the interaction between Nd<sup>3+</sup> ions and the LSB crystal lattice vibrations. The line broadening is caused by the direct one-phonon, multiphonon relaxation, and Raman scattering processes. Therefore, the width (in cm<sup>-1</sup>) of the *i*th energy level can be given by<sup>2</sup>

$$\Gamma_i = \Gamma_i^{\text{Strain}} + \Gamma_i^{\text{D}} + \Gamma_i^{\text{M}} + \Gamma_i^{\text{R}}, \quad (1)$$

where the first term,  $\Gamma_i^{\text{Strain}}$ , is the width due to the crystal strains; the second term,  $\Gamma_i^{\text{D}}$ , is the width due to direct one-phonon process between the *i*th energy level and other nearby *j* levels; the third term,  $\Gamma_i^{\text{M}}$ , is the contribution to the width from the multiphonon emission process; and the fourth term,  $\Gamma_i^{\text{R}}$ , represents the contribution to the spectral width due to

the Raman multiphonon process associated with phonon scattering by the impurity ions. The Raman scattering process consists of the absorption of one phonon and the emission of another phonon without changing the electronic state of the ion, and the width of the  $i$ th energy level. The temperature-dependent contribution of the one-photon process to the linewidth at the temperature range of our interest presented in this article is significant and is therefore included in our analysis. The total contribution to the linewidth due to microscopic strain, spontaneous one-phonon, and multiphonon emission processes is assumed to be temperature-independent. The net spectral width consisting of both the temperature-dependent and independent parts of the transition line is the sum of the energy spread of the two Stark energy levels involved in that particular transition, and can be written in the following form:<sup>2</sup>

$$\begin{aligned} \Gamma(T) = & \Gamma_0 + \sum_{j<i} \bar{\beta}_{ij} \frac{1}{e^{\frac{\Delta E_{ij}}{kT}} - 1} + \sum_{j>i} \bar{\beta}_{ij} \frac{1}{e^{\frac{\Delta E_{ji}}{kT}} - 1} + \sum_{j<f} \bar{\beta}_{fj} \frac{1}{e^{\frac{\Delta E_{fj}}{kT}} - 1} \\ & + \sum_{j>f} \bar{\beta}_{fj} \frac{1}{e^{\frac{\Delta E_{jf}}{kT}} - 1} + \bar{\alpha} \left( \frac{T}{\theta_D} \right)^7 \int_0^{\theta_D/T} \frac{x^6 e^x}{(e^x - 1)^2} dx, \end{aligned} \quad (2)$$

where  $\Gamma_0$  is the temperature-independent residual linewidth of the transition between the two levels and is due to random crystal strain and spontaneous one-phonon and multiphonon emission processes;  $\bar{\alpha}$ ,  $\bar{\beta}_{ij}$ , and  $\bar{\beta}_{fj}$  are the coupling coefficients for the ion-phonon interaction;  $E_i$  and  $E_f$  represent the initial and terminal energy levels, and  $E_j$  represents the intermediate energy level responsible for the phonon absorption or emission processes. For the initial level  $R_1$ , there is only one possible direct one-phonon absorption process ( $R_1 \rightarrow R_2$ ) for both transitions:  $R_1 \rightarrow Y_3$  and  $R_1 \rightarrow Z_4$ . It is difficult to determine all the coupling coefficients of  $\bar{\beta}_{ij}$  and  $\bar{\beta}_{fj}$ . For the  $R_1 \rightarrow Y_3$  transition, there is only one-phonon emission process ( $Y_3 \rightarrow Y_2$ ) and one-phonon absorption process ( $Y_3 \rightarrow Y_4$ ). Therefore, the theoretical temperature-dependent spectral width for the  $R_1 \rightarrow Y_3$  transition can be following simplified form:

$$\begin{aligned} \Gamma(T) = & \Gamma_0 + \bar{\beta}_{R_1 \rightarrow R_2} \frac{1}{e^{\frac{\Delta E_{R_1 \rightarrow R_2}}{kT}} - 1} + \bar{\beta}_{Y_3 \rightarrow Y_2} \frac{1}{e^{\frac{\Delta E_{Y_3 \rightarrow Y_2}}{kT}} - 1} + \bar{\beta}_{Y_3 \rightarrow Y_4} \frac{1}{e^{\frac{\Delta E_{Y_3 \rightarrow Y_4}}{kT}} - 1} \\ & + \bar{\alpha} \left( \frac{T}{\theta_D} \right)^7 \int_0^{\theta_D/T} \frac{x^6 e^x}{(e^x - 1)^2} dx, \end{aligned} \quad (3)$$

where  $\bar{\beta}_{R_1 \rightarrow R_2}$ ,  $\bar{\beta}_{Y_3 \rightarrow Y_2}$ ,  $\bar{\beta}_{Y_3 \rightarrow Y_4}$ ,  $\bar{\alpha}$ , and  $\theta_D$  are treated as adjustable parameters to obtain the best fitting for the experimental linewidth data.

For the  $R_1 \rightarrow Z_4$  transition, there is only one-phonon emission process ( $Z_4 \rightarrow Z_3$ ) and one-phonon absorption process ( $Z_4 \rightarrow Z_5$ ). Therefore, the temperature-dependent spectral width for the  $R_1 \rightarrow Z_4$  transition can be expressed in the following simplified form:

$$\begin{aligned} \Gamma(T) = & \Gamma_0 + \bar{\beta}_{R_1 \rightarrow R_2} \frac{1}{e^{\frac{\Delta E_{R_1 \rightarrow R_2}}{kT}} - 1} + \bar{\beta}_{Z_4 \rightarrow Z_3} \frac{1}{e^{\frac{\Delta E_{Z_4 \rightarrow Z_3}}{kT}} - 1} + \bar{\beta}_{Z_4 \rightarrow Z_5} \frac{1}{e^{\frac{\Delta E_{Z_4 \rightarrow Z_5}}{kT}} - 1} \\ & + \bar{\alpha} \left( \frac{T}{\theta_D} \right)^7 \int_0^{\theta_D/T} \frac{x^6 e^x}{(e^x - 1)^2} dx, \end{aligned} \quad (4)$$

where  $\bar{\beta}_{R_1 \rightarrow R_2}$ ,  $\bar{\beta}_{Z_4 \rightarrow Z_3}$ ,  $\bar{\beta}_{Z_4 \rightarrow Z_5}$ ,  $\bar{\alpha}$ , and  $\theta_D$  are treated as adjustable parameters to obtain the best fitting to the experimental linewidth data. The thermal broadening due to the direct one-phonon, multiphonon relaxation, and Raman phonon scattering processes is homogeneous and therefore yields a Lorentzian lineshape in the temperature range investigated.

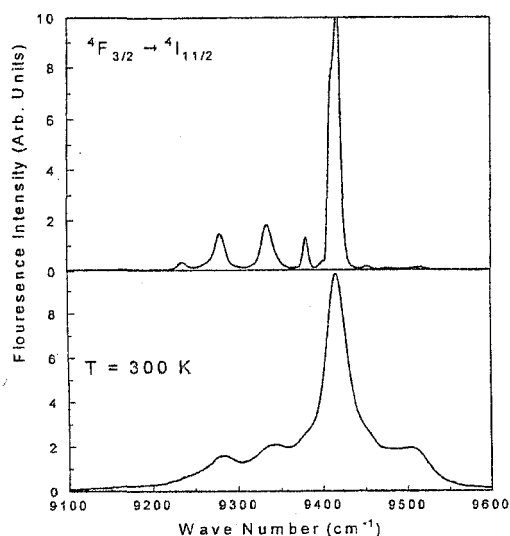


Figure 3. Fluorescence spectra at 10 K and 300 K for  ${}^4F_{3/2} \rightarrow {}^4I_{11/2}$  transition.

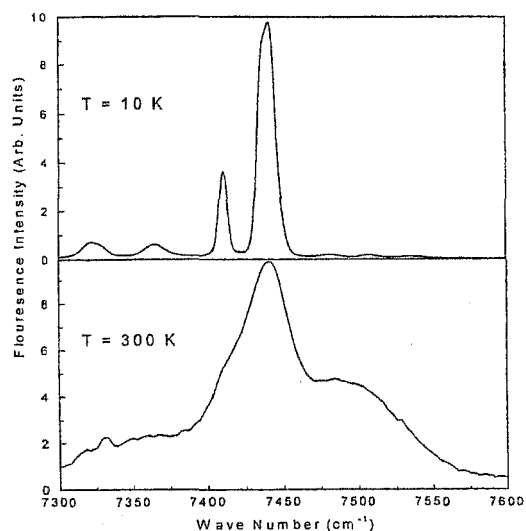


Figure 4. Fluorescence spectra at 10 K and 300 K for  ${}^4F_{3/2} \rightarrow {}^4I_{13/2}$  transition.

### Experimental Details

The fluorescence spectra were measured on  $\text{Nd}^{3+}$ :LSB in the temperature range of 10 - 300 K, by exciting the sample with the 514.5 nm line from a Spectra Physics model 2005 argon ion laser. Further experimental details can be found in Ref. 5.

For temperature-dependent studies, the spectroscopic sample of  $\text{Nd}^{3+}$ :LSB crystal was mounted at the cold finger of a CTI model 22, a closed-cycle helium cryogenic refrigerator, capable of varying temperature from 10 to 300 K. The temperatures were controlled by a Lake Shore model 320 temperature controller and measured by a silicon diode sensor attached to the sample holder.

### Results and Discussion

The emission spectra for the  ${}^4F_{3/2} \rightarrow {}^4I_{11/2}$  and  ${}^4F_{3/2} \rightarrow {}^4I_{13/2}$  transitions of  $\text{Nd}^{3+}$  in LSB have been taken at temperatures ranging from 10 to 300 K. The emission spectra of these transitions at 10 and 300 K are portrayed in Fig. 3 and 4, respectively. Figure 3 exhibits the most intense emission line at 1062 nm. The intensity of the 1062 nm line is about five times higher than those of the rest of the lines in Fig. 3. The intensity of the 1344 nm line is approximately three times

higher than those of the rest of the lines in Fig. 4. The temperature dependence of the line broadening and shift are clearly observed in these transitions. The strong, well-resolved inter-Stark transitions identified as  $R_1 \rightarrow Y_3$  at 1062 nm and  $R_1 \rightarrow Z_4$  at 1344 nm were measured at temperatures from 10 to 300 K. Using the fluorescence spectra of the  ${}^4F_{3/2} \rightarrow {}^4I_{11/2}$  and  ${}^4F_{3/2} \rightarrow {}^4I_{13/2}$  transitions of  $\text{Nd}^{3+}$  in LSB, the widths of the sharp lines of the  $R_1 \rightarrow Y_3$  and  $R_1 \rightarrow Z_4$  inter-Stark transitions have been investigated as a function of temperature. The shifts for the  $R_1 \rightarrow Y_3$  and  $R_1 \rightarrow Z_4$  were also measured as a function of temperature. The width (FWHM),  $\nu$  (in  $\text{cm}^{-1}$ ), of the 1062 nm line increased from  $14.7 \text{ cm}^{-1}$  at 10 K to  $35.5 \text{ cm}^{-1}$  at 300 K and the width of the 1344 nm line increased from  $13.3 \text{ cm}^{-1}$  at 10 K to  $59.7 \text{ cm}^{-1}$  at 300 K.

The linewidths of the  $R_1 \rightarrow Y_3$  and  $R_1 \rightarrow Z_4$  transitions were found to increase by 20.8 and  $46.4 \text{ cm}^{-1}$ , as the temperature was increased from 10 to 300 K. The experimental results have been quantitatively verified with the existing phonon-ion interaction theory that assumes the Debye phonon distribution in solids. The residual linewidths were estimated by extrapolating the experimental linewidth data to  $T = 0 \text{ K}$  and found to be  $14.61$  and  $13.27 \text{ cm}^{-1}$  for the  $R_1 \rightarrow Y_3$  and  $R_1 \rightarrow Z_4$  transitions, respectively.

The measured linewidths for the  $R_1 \rightarrow Y_3$  and  $R_1 \rightarrow Z_4$  transitions are plotted as a function of temperature in Fig. 5. The solid circles represent the experimental results and the solid curves are the theoretical fittings in these figures. The experimental linewidths data were best fitted to Eq. (3) and (4) with the fitting parameters given in Table I. The values of these parameters, along with Eqs. (3) and (4) can be used to recalculate the spectral linewidths (FWHM's) for both transitions, which are given in Table II.

**Table I.** Experimental linewidths ( $\Gamma$ ) and fitting parameters for the  $R_1 \rightarrow Y_3$  and  $R_1 \rightarrow Z_4$  transitions of  $Nd^{3+}$  in LSB.

Transition	Experimental		Fitting Parameters			
	$\Gamma$ (cm <sup>-1</sup> ) 10 K	$\Gamma$ (cm <sup>-1</sup> ) 300 K	$\theta_D$ (K)	$\alpha$ (cm <sup>-1</sup> )	$\beta$ (cm <sup>-1</sup> )	
$R_1 \rightarrow Y_3$	14.70	35.47	400.00	92.23	-6.36	$R_1 \rightarrow R_2$
					-11.24	$Y_3 \rightarrow Y_2$
					19.43	$Y_3 \rightarrow Y_4$
$R_1 \rightarrow Z_4$	13.28	59.73	400.00	248.33	-0.07	$R_1 \rightarrow R_2$
					-2.30	$Z_4 \rightarrow Z_3$
					11.16	$Z_4 \rightarrow Z_5$

According to the phonon theory,<sup>1</sup> thermal shift of a given transition is due to stationary effects of the phonon-ion interaction. In order to compare the experimental line shift, it is assumed that the thermal shift of a spectral line is the algebraic sum of the shifts of the two levels involved in the transitions. Therefore, the simplified theoretical expression for the line shift can be given in the following form:<sup>2</sup>

$$\delta\nu(T) = \delta\nu_0 + \alpha \left( \frac{T}{\theta_D} \right)^4 \int_0^{\theta_D/T} \frac{x^3}{e^x - 1} dx \quad (5)$$

where  $\delta\nu_0$  (in cm<sup>-1</sup>) =  $\nu(0 \text{ K}) - \nu(10 \text{ K})$  and  $\nu(0 \text{ K})$  was obtained by extrapolating the measured line position to absolute zero temperature.

The measured line shift for the  $R_1 \rightarrow Y_3$  (1062 nm) transition is plotted as a function of temperature in Fig. 6. The solid circles in Fig. 6 are the experimental data and the solid curve represents the theoretical fit. The measured line shifts have been best fitted to Eq. (5) with the fitting parameters given in Table III. However, the 1344 nm line was found to shift towards the shorter wavelengths with increasing temperature. The blue shift cannot be fitted with the existing theory. Although the so-called red shift is generally observed in most crystalline solids, the blue-shift is also reported in several crystals.<sup>6-9</sup>

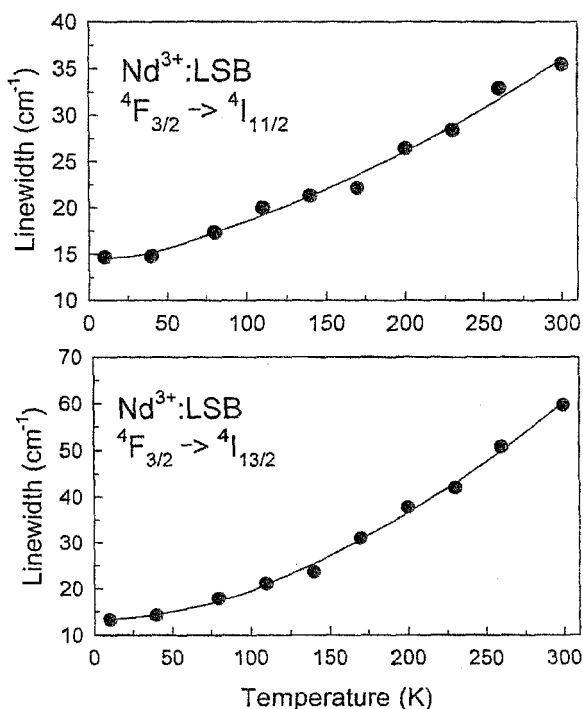


**Figure 5.** The linewidth for the  $R_1 \rightarrow Y_3$  and the  $R_1 \rightarrow Z_4$  transition of  $Nd^{3+}$  in LSB as a function of temperature.

**Table II.** Experimental and theoretical linewidths ( $\Gamma$ ) of the  $R_1 \rightarrow Y_3$  and  $R_1 \rightarrow Z_4$  transitions of  $\text{Nd}^{3+}$  in LSB at various temperatures and their deviations.

Temperature (K)	$\Gamma(R_1 \rightarrow Y_3)$ (cm <sup>-1</sup> )			$\Gamma(R_1 \rightarrow Z_4)$ (cm <sup>-1</sup> )		
	$\Gamma_{\text{exp}}$	$\Gamma_{\text{theo}}$	$\Delta\Gamma$	$\Gamma_{\text{exp}}$	$\Gamma_{\text{theo}}$	$\Delta\Gamma$
10	14.70	14.61	0.09	13.28	13.27	0.01
40	14.80	15.13	-0.33	14.19	14.37	-0.18
80	17.37	17.31	0.06	17.88	17.19	0.68
110	19.99	19.15	0.84	21.07	20.84	0.23
140	21.29	21.22	0.07	23.66	25.38	-1.72
170	22.14	23.52	-1.38	30.98	30.64	0.34
200	26.40	26.04	0.36	37.69	36.52	1.16
230	28.39	28.77	-0.39	41.99	42.98	-0.99
260	32.90	31.72	1.18	50.86	49.98	0.88
300	35.47	35.97	-0.50	59.73	60.13	-0.40

### Summary and Conclusion

We have shown that the phonon-ion interaction model accounts adequately for the temperature dependence of the linewidths of the  $R_1 \rightarrow Y_3$  and  $R_1 \rightarrow Z_4$  transitions of  $\text{Nd}^{3+}$  in LSB. The  $R_1 \rightarrow Y_3$  was found to shift towards the longer wavelengths (red shift) with increasing crystal temperature and was fitted with the existing theory. However, the  $R_1 \rightarrow Z_4$  spectral line has been observed to shift towards the shorter wavelengths (blue shift) with increasing crystal temperature and could not be fitted to the existing theory.

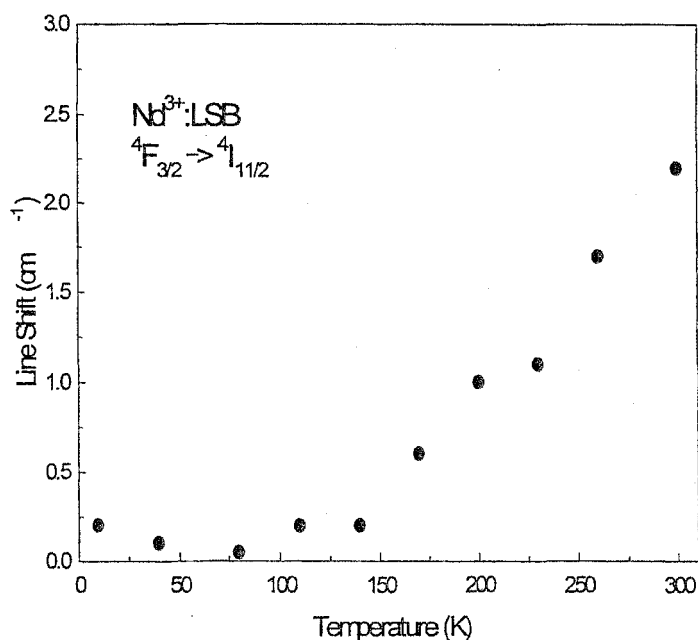


**Figure 6.** The line shift for  $R_1 \rightarrow Y_3$  as a function of temperature.

The fluorescence intensity of the 1062 nm line within the  ${}^4F_{3/2} \rightarrow {}^4I_{11/2}$  manifold remains almost the same at both 10 and 300 K. The linewidths of these transitions were found to remain reasonably small at room temperature. Since the threshold pumping power is directly proportional to the width of the laser line, it is imperative that the laser line has narrow width at the operating room temperature. This study, therefore, suggests that the spectral transitions investigated in  $\text{Nd}^{3+}$ :LSB can be suitable for efficient laser operation.

For the linewidths of  $R_1 \rightarrow Y_3$  and  $R_1 \rightarrow Z_4$  transitions, the best theoretical fittings were obtained with the same Debye temperature of  $\theta_D = 400$  K. It is important to note that the same Debye temperature was obtained for the best fitting of the temperature-dependent line shift for  $R_1 \rightarrow Y_3$  transition. Excellent agreements between the theoretical and experimental results are obtained over the entire temperature range after including the temperature-dependent direct one-phonon processes. Therefore, it may be concluded that the temperature-dependent part of the one-

**Table III.** Experimental line shift ( $\delta\nu$ ) and fitting parameters for the  $R_1 \rightarrow Y_3$  transition of  $Nd^{3+}$  in LSB.

Transition	Experimental	Fitting Parameters		
	$\delta\nu$ ( $cm^{-1}$ ) 10 – 300K	$\theta_D$ (K)	$\alpha$ ( $cm^{-1}$ )	$\delta\nu_0$ ( $cm^{-1}$ )
$R_1 \rightarrow Y_3$	-0.90	400.00	5.89	0.03

phonon process is of importance to the temperature dependence of linewidths of  $Nd^{3+}$ :LSB.

Although the spectral lines in crystalline solids are usually observed to shift toward the longer wavelengths (red shift) with increasing crystal temperature, in some crystals blue shifts have also been observed.<sup>2,3,6</sup> The red shifts of spectral lines could be fitted well with the theoretical expressions, while the blue shifts with increasing temperature could not be fitted with the available theoretical expression.<sup>2,6</sup> The blue shift of the  $R_1 \rightarrow Z_4$  transition can be attributed to the lowering of the terminal level of the transition due to the downward pushing by the upper Stark levels of the  $^4I_{13/2}$  manifold.<sup>4</sup> Nonetheless, the so-called “downward movement” of the lower level with increasing temperature is not clear yet. Therefore, more studies are required to further our understanding of this unusual process.

#### Acknowledgement

The authors would like to thank Thomas Reynolds at ReyTech Corporation for providing them with the crystal studied in this article. This research was supported by the National Science Foundation Grant No. DMR-0099479.

#### References

1. W. M. Yen, W. C. Scott, and A. L. Schawlow, *Phys. Rev.* **136**, A271 (1964).
2. X. Chen and B. Di Bartolo, *J. Appl. Phys.* **75**, 1710 (1994).
3. A. L. Schawlow, A. H. Piksis, and S. Sugano, *Phys. Rev.* **122**, 1469 (1961).
4. T. Kushida, *Phys. Rev.* **185**, 500 (1969).
5. D. K. Sardar and S. C. Stubblefield, *Phys. Rev. B* **60**, 14724 (1999); *J. Appl. Phys.* **83**, 1195 (1998), and references therein.
6. D. K. Sardar and R. M. Raylon, *J. Opt. Mater.*, **14**, 5 (2000).
7. D. K. Sardar, F. S. Salinas, and R. M. Yow, *J. Appl. Phys.* **88**, 4688 (2000).
8. D. K. Sardar, R. M. Yow and A. Sayka, *Phys. Stat. Solid (b)* **223**, 691 (2001).
9. B. Di Bartolo, *Optical Interactions in Solids*, (Wiley, New York, 1968), p. 341.